Rare Metal Materials and Engineering
Volume 47, Issue 6, June 2018
Online English edition of the Chinese language journal

Available online at www.sciencedirect.com

Cite this article as: Rare Metal Materials and Engineering, 2018, 47(6): 1662-1667.

ARTICLE

H Isotope Effects in $^{6,7}LiX$ (X=H, D, T)+H_2O Deliquescence Reactions: a Quantum Chemistry Study

Li Rusong[1], **Liu Zhiyong**[2], **Xin Duqiang** [1], **Wang Zhen**[1]

[1] *Xijing University, Xi'an 710123, China;* [2] *Beijing Research Institute of High Technology, Beijing 100084, China*

Abstract: We performed theoretical investigation on mechanisms of LiD/LiH/LiT+H_2O reactions with second order perturbation theory (MP2). Calculations of enthalpy change and reaction rate constant are in agreement with experimental data and other theoretical values. Results show that two reaction channels exist for LiD+H_2O reaction, and channel 1 is the main reaction channel. Kinetic Isotope Effect (KIE) is not so large although fracture of isotope bond takes place in the reaction, which is noticeably different from theoretical maximums of primary isotope effect. Individual contributions of KIE effect are listed as follows $\eta_{vib}>\eta_{rot}>\eta_{tun}>\eta_{pot}>\eta_{trans}$, indicating that main contribution of isotope effect results from vibration factor.

Key words: isotope effect; reaction channel; vibration frequency; transition state; rate constant

^{6}LiD is an important fusion fuel which is characterized by $^6Li+n \rightarrow T+^4He$ and $D+T \rightarrow n+^4He$, so it is widely applied in fusion reaction. However, LiD has usually strong chemical activity, and is apt to react with H_2O, CO_2 and O_2 in air, for example, reaction of H_2O with LiD will form LiOH and LiOD, of which chemical reaction is given by[1] $2LiD(s)+2H_2O(g)=LiOH(s)+LiOD(s)+H_2(g)+HD(g)$.

Powder of these materials can ignite in humid air, and sometimes dust explosion occurs. Moreover, bulk materials can combust with exterior ignition source. In addition, these materials readily react with other organic dissolvent, such as ethanol and ether. These reactions make them deliquescence, deterioration and degradation, and the products LiOH(D, T) is an alkali, and have strong corrosiveness [2]. This deliquescence process might gradually deteriorate physical grade, thus making them dissatisfy requirement (therefore “retirement”). Therefore, surface of LiX material are often painted a thin moisture barrier; it just weakens deliquescence process, and it amounts to deliquesce at a very low relative humidity since moisture penetrability of moisture barrier is non-negligible.

Experimentally, great attentions have been paid on the aging mechanisms of protective layer for LiH. Previous reports have demonstrated that initially LiH reacts with moisture to generate LiOH layer in moist air, then LiOH slowly reacts with other LiH to produce Li_2O and H_2, and finally forms LiOH or Li_2O layers on LiH surface. LiOH is inclined to produce LiOH·H_2O when exposed to moist air with >15% relative humidity [3,4]. Li et al. [1] have investigated reaction kinetics of LiD powder with O_2, CO_2 and water vapor, and showed that LiD slightly reacts with O_2 and CO_2, in contrast to relatively large reaction rate for water vapor. Dinh et al. [5] have adopted a temperature programme method to study decomposition process of LiOH and its corrosion rate in presence of water vapor, and analyzed possible corrosion mechanisms for LiH oxidation[6,7]. Xu et al. [8] have used a quadratic configuration interaction method (QCISD) and coupled cluster singles and doubles theory (CCSD) to investigate ground state geometry and potential function of LiH molecule. Luo et al. [3] have optimized geometry of LiH molecule on the basis of relativistic effective core potential (RECP) and hybrid density functional B3LYP method. Xie et al.[9] have adopted singlet closed-shell configuration interaction method (SAC-CI method) to optimize equilibrium geometries and harmonic frequencies of ground state $X^1\Sigma^+$, the first excited state $A^1\Sigma^+$ and the second degenerate excited state $B^1\Pi$ of LiH molecule with D95(d), 6-311G** and cc-PVTZ

Received date: June 14, 2017
Foundation item: National Natural Science Foundation of China (51401237, 51271198, 11474358); Defence Foundation of China ([2014]689, 2015ZZDJJ02, 2014QNJJ018, YX2012cxpy06)

Corresponding author: Li Rusong, Ph.D., Associate Professor, Xijing University, Xi'an 710123, P. R.China, Tel: 0086-29-85628017, E-mail: 20170213@xijing.edu.cn

base sets. They also have used Group Sum of Operator method (GSUM) to perform single point energy calculations of two excited states ($A^1\Sigma^+$ and $B^1\Pi$), fit the energy data with a canonical equation, and have indicated that potential functions of electronic states are in good agreement with experimental data. Lei et al. [10,11] have studied possible reactions of Li*X* (*X*=H, D, T) with H_2O, and calculated configuration parameters, vibration frequencies and energies of various stationary points on the minimum potential surface of reactive system, and corresponding reaction rate. Moreover, they have performed density functional theory study on thermodynamics properties of LiD as a function of temperature and pressure under high temperature and pressure [12,13]. Xiao have theoretically derived hydrolysis rate equation for LiH at low-humidity condition[14]. Stwalley et al. have identified and reviewed experimental measurements and many theoretical calculations of spectroscopy and structure of isotopic lithium hybrides (^{6}LiH, ^{7}LiH, ^{6}LiD, ^{7}LiD), and reported dissociation energies for various electronic states[15]. Vidal et al. have determined the molecular constants and their adiabatic corrections for isotopic lithium hydrides (^{6}LiH, ^{7}LiH, ^{6}LiD and ^{7}LiD)[16]. Pan et al. calculated six normal mode vibration frequencies and infrared intensities for three tetra-atomic Li-H ion clusters have been calculated using SCF, MP2, and CISD methods [17]. Ramzan et al. reported ab initio molecular dynamics calculations based on density functional theory to study the hydrogen-deuterium exchange in LiH, and predicted the single hydrogen-deuterium exchange and self-diffusion constants in LiH [18]. Dologlou obtained the temperature dependence of the diffusion coefficients of hydrogen and deuterium in LiH in terms of a thermodynamical model [19].

To the best of our knowledge, there is little theoretical investigation on ^{6,7}Li*X* (*X*= H, D, T) + H_2O deliquescence reaction since Li*X* reaction behaviors and mechanisms under H_2O atmosphere are very complicated. However much attention have been paid on experimental aspects of Li*X* hydrolysis process. In fact, D (T) substitution of H may dramatically changes physical and thermodynamical properties of Li*X*, such as entropy and enthalpy. A main purpose of this work is to capture microscopic mechanisms for these chemistry reactions which are crucial to understand this complicated reaction system. In addition, we first study equilibrium and dynamics isotope effects for D (T) substitution of H.

1 Computational Details

In this work we adopt a perturbation theory method MP2/6-311G(d) to optimize structural configurations of reactant, chemical intermediate, transition state and product, and verify transition state in term of frequency analysis. Usually 6-311G(d) basis function is used for structural optimization, and 6-311++G** basis function for single-point energy calculation. Relative energies of transition state and product to reactant, and Eqs.(1)~(3) can yield enthalpy change, Gibbs energy change and entropy change for reaction control step[20,21]

$$\Delta_r^{\neq} H_m = H_{TS} - H_R \tag{1}$$

$$\Delta_r^{\neq} G_m = G_{TS} - G_R \tag{2}$$

$$\Delta_r^{\neq} S_m = \frac{\Delta_r^{\neq} H_m - \Delta_r^{\neq} G_m}{T} \tag{3}$$

where, $\Delta_r^{\neq} H_m$, $\Delta_r^{\neq} G_m$ and $\Delta_r^{\neq} S_m$ denote enthalpy change, Gibbs free energy change and entropy change, respectively.

Reaction rate constant is defined as Eq.(4) by classical transition state theory [22] with quantization correction taken into account

$$k = A e^{-E_a/RT} \tag{4}$$

where E_a is reaction activation energy, which is defined as energy difference (corrected by zero-point energy) between transition state and chemical intermediate or reactant.

Existence of isotopes can result in equilibrium constant difference, so called Equilibrium Isotope Effect (EIE), which numerically equals to ratio of equilibrium constant for lighter isotope to that of heavier isotope and is dependent on equilibrium isotope effect and ΔG of reactant[23-26]

$$\frac{K_{light}}{K_{heavy}} = e^{-\frac{\Delta G_{light} - \Delta G_{heavy}}{RT}} \tag{5}$$

here ΔG denotes free energy change from reactant to product.

In addition, existence of isotopes would lead to reaction rate difference, so called Kinetic Isotope Effect (KIE), of which general form is written as[25,26]

$$\eta = \eta_{tun}^{TST} \eta_{PF}^{TST} \tag{6}$$

$$\eta_{tun}^{TST} = \Gamma_U^W / \Gamma_S^W \tag{7}$$

$$\eta_{PF}^{TST} = \frac{Q_U^{\neq} / Q_U^R}{Q_S^{\neq} / Q_S^R} \tag{8}$$

where η_{tun}^{TST} and η_{PF}^{TST} are contributions of tunnel effect (tun) and partition function (PF) to KIE effect, respectively. $Q_S^{\neq}$ ($Q_U^{\neq}$) and Q_S^R (Q_U^R) represent partition functions of transition state and reactant when H is (un) substituted by D or T.

$$\Gamma^W = 1 - \frac{(hV^{\neq}/k_B T)^2}{24} \tag{9}$$

where $V^{\neq}$ denotes potential energy of transition state, k_B and T is Boltzmann constant and thermodynamic temperature, respectively.

On basis of canonical variation transition theory (CVT), Eq.(6) can be rewritten as

$$\eta = \eta_{tun} \eta_{PF} \eta_{pot} \tag{10}$$

$$\eta_{tun} = \Gamma_U^{CVT} / \Gamma_S^{CVT} \tag{11}$$

$$\eta_{PF} = \frac{Q_U^{CVT} / Q_U^R}{Q_S^{CVT} / Q_S^R} \tag{12}$$

$$\eta_{pot} = \exp\left[-\beta(V_U^{CVT} - V_S^{CVT})\right] \tag{13}$$

In fact, η_{elec} term is not included in above formulas since electronic partition function would not be influenced by isotope substitution[27].

We optimize molecular geometries of individual stationary points for LiH/LiD/LiT+H_2O corrosion reactions with perturbation method MP2 at 6-311G(d) level, determine reaction intermediate and transition state in term of frequency analysis, and calculate intrinsic reaction coordination (IRC) to confirm validity of transition state. At the same time we calculate energies of reactant, chemical intermediate, transition state and product at CCSD/6-311++G(d, p) level based on optimization results, and compare relative energies of every matters, so as to improve the precision and save the computational resource. CCSD is a coupling cluster method with electron correlation effect which is practically viewed as an extension of HF method. Unfortunately, HF method cannot adequately capture electron correlation effect, especially instantaneous electron correlation interaction, and cannot give good description of a system with remarkable electron correlation effect; however it can provide a valid model for many systems. Thus, Eqs.(1)~(5) and CCSD method can be used to obtain mole enthalpy changes (namely thermal effect) and reaction rate constants for following reactions.

Two following reaction channels for LiD+H_2O reaction have been studied at CCSD/6-311++G(d,p)//MP2/6-311G(d) level

$LiD+H_2O \rightarrow LiOH+HD$ (channel 1)

$LiD+H_2O \rightarrow LiOD+H_2$ (channel 2)

Reaction rate constants of these two reaction channels calculated with Arrenhnius formula show that above reactions are apt to form LiOH and HD.

Like LiD, T would take the place of H in LiH, and LiT+H_2O reaction also has two channels

$LiT+H_2O \rightarrow LiOH+HT$ (channel 1')

$LiT+H_2O \rightarrow LiOT+H_2$ (channel 2')

As discussed below, calculation results show that there are absence of chemical intermediate and transition state, and a single channel exists for the reaction. Reaction rate constants of two channels for LiH/LiT+H_2O calculated with Arrenhnius formula can be used to shed light on LiH/LiD/LiT + H_2O reaction mechanisms. We only consider the first reaction channel for LiD isotope effect since the second channel is much smaller compared to the first one. For brevity, we denote three channels for LiH/LiD/LiT+H_2O reactions as R1/R2/R3.

2 Results and Discussion

2.1 Mechanism of LiD+H_2O reaction

Table 1 presents zero-point energies (ZPE) of individual stationary points for reactive system, including zero-point energies at MP2/6-311G(d)/CCSD/6-311++G(d,p) levels, and relative energies with reference to reactant energies at CCSD-ZPE level E_{rel}. Energy level changes for LiD + H_2O reaction are plotted in Fig.1. Potential barriers for each reaction channel and enthalpy changes at room temperature (298 K) ΔH) is listed in Table 2. From Fig.1 we can see that product energies of two reactions are both smaller than those of reactants, which indicates that product energies of exothermic process are at least 40 kJ·mol^{-1} smaller than those of reactants, and both channels are thermodynamicallyprobable reactions.

Table 1 Total energies, zero-point energies and relative energies ΔE of individual stationary points for LiD+H_2O reaction (kJ·mol^{-1})

Reactant	E(MP2)	E(ZPE)	E(CCSD)	E(CCSD+ZPE)	ΔE
LiD+H_2O	–84.2362737	0.024334	–84.2976723	–84.2733383	0.00
M1	–84.2768153	0.027547	–84.3276009	–84.3000539	–70.1413636
TS1	–84.2682742	0.023896	–84.3212304	–84.2987914	–60.8266908
LiOH + HD	–84.2938067	0.021184	–84.3445801	–84.3233961	–131.425922
TS2	–84.156838	0.021387	–84.2204263	–84.1990393	195.077891
M2	–84.1572348	0.021315	–84.2208779	–84.1995629	193.696086
TS3	–84.1568384	0.020037	–84.2104315	–84.1903945	217.765678
M3	–84.2768152	0.025202	–84.3275692	–84.3023672	–76.2148943
TS4	–84.2682732	0.022511	–84.3212072	–84.2986962	–66.57674482
LiOD+H_2	–84.2938067	0.019956	–84.3445801	–84.3246241	–134.6500152

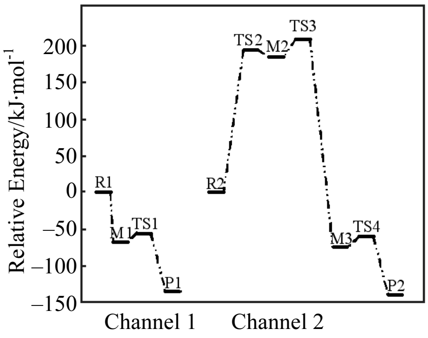

Fig.1 Relative energies of reactant, chemical intermediate, transition state and product in each reaction channel for LiD+H_2O reaction

As shown in Table 1, chemical intermediate M1 formed by O in H_2O bonding with Li in LiD has the minimal energy, rather than D in LiD. There are substantially no changes for Li(3)-D(2) and O(1)-H(4,5) bonds in M1, indicating that approach of two atoms immediately forms stable intermediate. This reaction is absence of activation energy, and releases heat quantity of 70.1 kJ·mol^{-1}, which promotes vibration frequency increase of intermediate M1 and further results in isomerization. O(1) atom bonds with Li(3) atom and forms transition

Table 2 Energies barriers ΔE and enthalpy changes ΔH of each reaction channel for LiD+H_2O reaction

Initial state	Reach state	ΔE/kJ·mol^{-1}		ΔH^{a}/kJ·mol^{-1}
		MP2/6-311G(d)	CCSD/6-311++G(d, p)	
LiD+H_2O	M1	–106.44	–78.57	–100.13
M1	TS1	22.42	16.72	8.87
TS1	LiOH+HD	–67.04	–61.30	–67.25
LiD+H_2O	TS2	208.56	202.81	194.74
TS2	M2	–1.04	–1.19	–2.31
M2	TS3	1.04	2.74	5.79
TS3	M3	–314.99	–307.54	–297.31
M3	TS4	22.42	16.70	11.26
TS4	LiOD+H_2	–67.04	–61.37	–66.70

[a] MP2/6-311G(d) calculation results

state TS1 since Li is more apt to lose outermost electrons. Li(3)-D(2) and O(1)~H(5) bonds in TS1 state obviously stretch and transfers of H atom occur, while untransferred H(4) atom is almost in line with O(1) and Li(3) atoms, and length of Li(3)-O(1) bond shortens about 10%. Comparison of M1 and TS1 configurations shows that Li(3)-D(2) bond gradually stretches and D(2) approaches H(5) after forming of chemical intermediate (activation energy of this reaction is only 19.75 kJ·mol^{-1}). Extension vibration frequency of Li(3)-D(2) bond is enhanced as transition state TS1 vibrates. Li(3)-D(2) and O(1)-H(5) bonds further extend, resulting in complete fracture of these two bonds, while D(2) atom gradually gets close to H(5) atom and finally forms P1 product (LiOH and HD). The reaction spontaneously proceeds since activation energy of this channel control procedure is only 9.315 kJ·mol^{-1}. Comparison between energy of reactant with that of product indicates that the reaction simultaneously releases a great deal of heat, showing that it is an exothermic reaction (reaction heat is 131.4 kJ ·mol^{-1}).

As shown in Fig.1, reaction mechanism of channel 1 is more complicated than that of channel 2, which undergoes TS2, M2, TS3, M3 and TS4 transition states, and finally forms P2(LiOD and H_2). As a matter of fact, we can divide reaction channel 2 into two parts. In the first part reactants mutually approach, absorb a certain amount of heat, undergo a higher potential barrier and forms TS2 transition state. Then TS2 state releases a small amount of heat to reach a stationary point M2 with somewhat lower energy, and passes through a potential barrier of 24.1 kJ·mol^{-1} to form TS3 state. From TS2, M2 and TS3 states we can see that configurations of these three stationary points are very similar to each other, displaying a cone-like structure. D(2), H(4), H(5) and O(1) atoms are approximately in the same plane, of which O(1) atom is located in the center, while the other three atoms are uniformly distributed around O(1) atom. There are tiny energy differences for TS2, M2 and TS3 stationary points, and O(1)-Li(3) bond nearly maintains invariant; however bonds of D(2), H(4) and H(5) atoms with O(1) atom obviously change. Lengths of O(1)-D(2), O(1)-H(4) and O(1)-H(5) bonds in TS2 state are 0.1129, 0.1035, 0.1035 nm. 0.1055, 0.1053 and 0.1053 nm in M2 state, and 0.1035, 0.1131 and 0.1034 nm in TS3 state, respectively. Apparently, this process is an adjustment of bond length or a transfer of H atom, which is amount to interchange of D(2) and H(4) positions. In the second part O(1)-H(4) bond is longer than O(1)-D(2) and O(1)-H(5) bonds once TS3 state forms. O(1)-H(4) bond continuously stretches, leads to complete fracture of the bond, and forms stable chemical intermediate M3 with increase of vibration frequency. The reaction releases 324.2 kJ·mol^{-1}, which prompts enhancement of internal vibration. O(1)-H(5) and Li(3)-H(4) bonds gradually extend and break down, while H(4) atom gets close to H(5) atom and forms TS4 state. At the same time, two H atoms gradually approach to each other and finally form P2. By comparison to channel 1, M3 configuration (also energy) is similar to M1 configuration.

2.2 Mechanisms of LiH/LiT+H_2O reactions

Table 3 lists ZPE of individual stationary points for the reactive system, including zero-point energies at MP2/6-311G(d)

Table 3 Total energies, zero-point energies and relative energies ΔE of stationary points for LiH/LiT+H_2O reaction channels (kJ·mol^{-1})

Initial state	E(MP2)	E(ZPE)	E(CCSD)	E(CCSD+ZPE	ΔE
LiH+H_2O	–84.2111427	0.025131	–84.2897332	–84.2646022	0.00
M1	–84.2483937	0.028421	–84.3275914	–84.2991704	–90.7582343
TS1	–84.2427023	0.025470	–84.3212316	–84.2957616	–81.8084866
LiOH+H_2	–84.2711287	0.022678	–84.3445801	–84.3219021	–150.4399347
LiT+H_2O	–84.2122697	0.024004	–84.2976723	–84.2736190	–23.6734585
M2	–84.2496887	0.027126	–84.3275914	–84.3004654	–94.1582353
TS2	–84.2450382	0.023236	–84.3199207	–84.2966847	–84.2309995
LiOH+HT	–84.2729887	0.020818	–84.3445801	–84.3237621	–155.3233338

and CCSD/6-311++G** levels, and relative energies with reference to reactant energies at CCSD-ZPE level $E_{\rm rel}$. Potential barriers for each reaction channel and enthalpy changes at room temperature (298 K) ΔH) is listed in Table 2. Reaction mechanism plot for $LiH+H_2O \rightarrow LiOH+H_2$ is presented in Fig.2.

As shown in Fig.2, reaction mechanism for $LiH+H_2O$ is as follows. Li atom will bond with O atom and form stable chemical intermediate M1 with distance of LiH and H_2O molecules reaching a certain value. Length of O-H bond in H_2O nearly maintains invariable, while bond length of Li(1)-H(2) increases from 0.16076 nm to 0.16338 nm. This procedure is free of threshold energy, and releases heat of 90.8 kJ·mol^{-1}, which promotes chemical intermediate to strongly vibrate and gradually transform into transition state TS1. Li(1)-H(2) and O(3)-H(5) bonds in TS1 state elongate from 0.16338 and 0.09577 nm to 0.17951 and 0.11817 nm, respectively, indicating occurrence of H transfer. However immobile H and O atoms are almost in line with Li atom, and Li(1)-O(3) bond length changes from 0.19094 nm to 0.17592 nm. Thus, this procedure is the control step for entire reaction (activation energy is only 8.95 kJ·mol^{-1}, which is consistent with 10.37 kJ·mol^{-1} in Ref.[11]), theoretically verifying it is a spontaneous reaction for $LiH+H_2O$ reaction. It is known that bonds in transition state are unstable, so Li(1)-H(2) and O(3)-H(5) bonds gradually stretch and completely break up with enhancement of internal vibration in transition state. Then H(2) and H(5) atoms break away from complicated compound, get close to each other, and form reactive product (LiOH and H_2). This process releases heat of 68.63 kJ·mol^{-1}, and reaction heat of whole reaction process is 150.44 kJ·mol^{-1}. Reaction mechanism of $LiT+H_2O \rightarrow LiOH+HT$ is almost the same as that of $LiH+H_2O \rightarrow LiOH+H_2$.

2.3 H isotope effect

Vibration frequencies for various vibration modes of transition states in R1~R3 reactions are presented in Table 4 (only lists six vibration frequencies in relation to D/T isotope substitution). Equilibrium rates show that $\nu_{\rm R1} > \nu_{\rm R2} > \nu_{\rm R3}$, which is consistent with activation energy sequence $E_{\rm a,R1} < E_{\rm a,R2} < E_{\rm a,R3}$.

Replacement of H with D/T will affect vibration frequencies of transition states (Table 4), and six vibration frequencies in relation to this replacement will in turn decrease. However irrelevant vibration frequencies almost maintain invariant, which is the major cause of KIE effect.

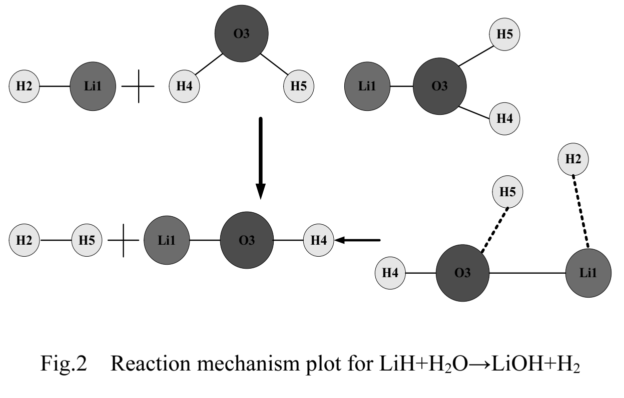

Fig.2 Reaction mechanism plot for $LiH+H_2O \rightarrow LiOH+H_2$

Table 4 Vibration frequencies of vibration modes for various transition states in R1~R3 reactions (cm^{-1})

Vibration mode	$\nu_{\rm R1}$	$\nu_{\rm R2}$	$\nu_{\rm R3}$
1	–1313.5	–1272.4	–1254.2
2	653.1	628.5	598.0
3	762.2	715.5	668.3
4	866.7	756.3	746.5
5	1369.9	1102.0	937.6
6	1502.2	1286.4	1258.5

As shown in Table 4, we address the following contributions of various factors to KIE effect: (i) Tunnel effect. η value is small since vibration frequencies of imaginary frequency modes for transition states in these three reactions are close to each other, where $\eta_{\rm tun}^{\rm TST}$ is approximately equal to $\eta_{\rm tun}^{\rm CVG}$, resulting in smaller contribution of tunnel effect. (ii) Translation effect. $\eta_{\rm trans,R2}$ and $\eta_{\rm trans,R3}$ have negative contribution to η (<1). (iii) Rotation effect. Contribution of rotation effect is dependent on structures of reactants and transition states. It is shown that their structures are practically similar to each other, so rotation component has a tinyeffect on η. (iv) Vibration effect. As mentioned before, isotope substitution has an apparent effect on vibration frequencies of various stationary points. η values of R2 and R3 reactions are 2.41 and 2.79, respectively, which are the major cause of KIE effect.

3 Conclusion

We perform theoretical investigation on mechanisms of $LiD/LiH/LiT+H_2O$ reactions with MP2 method, optimize chemical intermediates and transition states, and prove transition states to be on the correct reaction channel using intrinsic reaction coordination method. EIE and KIE effects of R2 and R3 reactions at room temperature (298 K) have been calculated with variation transition state theory and corresponding tunnel correction. Calculation results show that KIE effect is not so large although fracture of isotope bond takes place in the reaction (belongs to primary isotope effect), namely $\eta_{\rm H/D}$=2.35, $\eta_{\rm H/T}$ =2.65, which are noticeably different from theoretical maximums of primary isotope effect ($\eta_{\rm H/D}$=6.5, $\eta_{\rm H/T}$=14.58). In various contributions of KIE effect $\eta_{\rm vib} > \eta_{\rm rot} > \eta_{\rm tun} > \eta_{\rm pot} > \eta_{\rm trans}$, indicating that main contribution of isotope effect results from vibration factor. Frequencies of vibration mode in relation to isotope substitution remarkably decrease, giving rise to change of KIE effect.

References

1 Li G, Lu G D, Jing W Y *et al*. *Journal of Nuclear and Radiochemistry*[J], 2004, 26: 99 (in Chinese)

2 Luo J T. *Strength & Environment*[J], 1992, 88: 54 (in Chinese)

3 Luo D L, Meng D Q, Zhu Z H. *Acta Physica Sinica*[J], 2003, 52:

2438 (in Chinese)
4 Zhu Z Y, Zhu Z H, Zhang L *et al*. *Acta Physica Sinica*[J], 2011, 60: 123102 (in Chinese)
5 Dinh L N, Cecala C M, Leckey J H *et al*. *Journal of Nuclear Materials*[J], 2001, 295: 193
6 Dinh L N, Grant D M, Schildbach M A *et al*. *Journal of Nuclear Materials*[J], 2005, 347: 31
7 Plummer G M, Herbst E, De Lucia F C. *Journal of Chemical Physics*[J], 1984, 81: 4893
8 Xu M, Ling-hu R F, Wang R K *et al*. *Journal o f Guizhou Normal University, Natural Sciences*[J], 2007, 25: 56 (in Chinese)
9 Xie A D, Shi D H, Zhu Z L *et al*. *Chinese Journal of Chemical Physics*[J], 2005, 18: 776 (in Chinese)
10 Lei J H, Duan H, Xing P F *et al*. *Atomic Energy Science and Technology*[J], 2011, 45: 1165 (in Chinese)
11 Lei J H, Xing P F, Tang Y J *et al*. *High Power Laser and Particle Beams*[J], 2010, 22: 2308 (in Chinese)
12 Duan T, Lei J H, Tang Y J. *Atomic Energy Science and Technology*[J], 2011, 45: 394 (in Chinese)
13 Lei J H, Xing P F, Tang Y J *et al*. *Progress Report on China Nuclear Science & Technology*[R], Beijing: Chinese Nuclear Society, 2009, 1: 16 (in Chinese)
14 Xiao S, Shuai M B, Chu M F. *Materials Review*[J], 2010, 24: 321 (in Chinese)
15 Stwalley W C, Zemke W T. *Journal of Physical and Chemical Reference Data*[J], 1993, 22: 87
16 Vidal C R, Stwalley W C. *Journal of Chemical Physics*[J], 1982, 77: 883
17 Pan Z F, Barkman R. F. *Journal of Chemical Physics*[J], 1994, 101: 7782
18 Ramzan M, Ahuja R. *Journal of Applied Physics*[J], 2009, 106: 016 104
19 Dologlou E. *Journal of Applied Physics*[J], 2010, 107: 083 507
20 Zhong Z K, Zhang L, Sun Y *et al*. *Atomic Energy Science and Technology*[J], 2015, 49: 250 (in Chinese)
21 Zhu Z H, Yu H G. *Molecular Structure and Molecular Potential Function*[M]. Beijing: Science Press, 1997 (in Chinese)
22 Li B Z. *Chinese Journal of Chemical Physics*[J], 2004, 17: 433 (in Chinese)
23 Luo W L, Ruan W, Zhang L *et al*. *Acta Physica Sinica*[J], 2008, 57: 4833 (in Chinese)
24 Zhang L, Zhong Z K, Zhu Z Y *et al*. *Chinese Journal of Chemical Physics*[J], 2003, 16: 455 (in Chinese)
25 Wang R, Zhang L, Jiang G *et al*. *Nuclear Physics Review*[J], 2009, 26: 150
26 Wang Y M, Wang Y L, Tian J. *Chemistry of University*[J], 2004, 19: 32 (in Chinese)
27 Cao X Y, Li Z H. *Chinese Journal of Chemical Physics*[J], 1997, 10: 364 (in Chinese)

^{6,7}LiX (X=H, D, T)+H_2O 潮解反应过程中氢同位素效应：量子化学研究

李如松[1]，刘志勇[2]，辛督强[1]，王　震[1]
(1. 西京学院，陕西 西安 710123)
(2. 北京高新技术研究所，北京 100084）

摘　要：采用二阶微扰方法 MP2 对 LiD/LiH/LiT+H_2O 反应机制进行理论，计算获得的焓变化和反应速率常数与实验数据和其他理论值一致。结果表明：LiD+H_2O 反应存在 2 个反应通道，通道一的反应势垒仅为 9.31 kJ/mol，并且通道一是主要的反应通道。平衡同位素效应 EIE 和动力学同位素效应 KIE 计算结果表明：虽然反应中同位素化学键发生破裂，属于主级同位素效应，但是动力学同位素效应不是非常明显，这与主级同位素效应的理论极大值不同。在动力学同位素效应的贡献中 $\eta_{vib}>\eta_{rot}>\eta_{tun}>\eta_{pot}>\eta_{trans}$，这表明同位素效应的主要贡献来自振动因子，发生同位素效应替代后，与之相关的振动模式的振动频率明显降低，引起 KIE 的变化。

关键词：同位素效应；反应通道；振动频率；过渡态；反应速率

作者简介：李如松，男，1983 年生，博士，副教授，西京学院，陕西 西安 710123, E-mail: 20170213@xijing.edu.cn